

ChemComm

Accepted Manuscript



This is an *Accepted Manuscript*, which has been through the Royal Society of Chemistry peer review process and has been accepted for publication.

Accepted Manuscripts are published online shortly after acceptance, before technical editing, formatting and proof reading. Using this free service, authors can make their results available to the community, in citable form, before we publish the edited article. We will replace this *Accepted Manuscript* with the edited and formatted *Advance Article* as soon as it is available.

You can find more information about *Accepted Manuscripts* in the [Information for Authors](#).

Please note that technical editing may introduce minor changes to the text and/or graphics, which may alter content. The journal's standard [Terms & Conditions](#) and the [Ethical guidelines](#) still apply. In no event shall the Royal Society of Chemistry be held responsible for any errors or omissions in this *Accepted Manuscript* or any consequences arising from the use of any information it contains.

COMMUNICATION

A 3D MOF showing unprecedented solvent-induced single-crystal-to-single-crystal transformation and excellent CO₂ adsorption selectivity at room temperature

Cite this: DOI: 10.1039/x0xx00000x

Received 00th January 2012,
Accepted 00th January 2012

DOI: 10.1039/x0xx00000x

www.rsc.org/

Tao Qin,^{‡a} Jun Gong,^{‡a} Junhan Ma,^a Xin Wang,^a Yonghua Wang,^b Yan Xu,^a Xuan Shen^a and Dunru Zhu^{*a}

A water stable porous 3D metal-organic framework, [Cu₃L₂(μ₃-OH)₂(μ₂-H₂O)]·2DMA (1, mother crystal, H₂L = 2,2'-dinitrobiphenyl-4,4'-dicarboxylic acid, DMA = *N,N*-dimethylacetamide) shows unprecedented irreversible solvent-induced substitutions of bridging aqua ligands and guest-exchanges in single-crystal-to-single-crystal (SCSC) transformations at room temperature (RT), producing quantitatively three daughter crystals, [Cu₃L₂(μ₃-OH)₂]·2S (2: 2A, S = acetone; 2B, S = 2-propanol; 2C, S = 2-butanol) which exhibit reversible interconversion by guest-exchanges at RT in SCSC transformations. MOF 1 shows excellent separation selectivity (128) of CO₂/N₂ at RT and is a better sorbent of micro-solid-phase extraction (μ-SPE) than currently known benchmark ZIF-8.

Metal-organic frameworks (MOFs) have gained increasing attention due to their variety of topological architectures¹ and potential applications in gas storage, separation, and catalysis.² Among crystalline MOFs, SCSC transformation is a particularly interesting phenomenon that has attracted considerable attention in recent years since the process can directly provide the accurate relationship between the structures and properties.³ In general, SCSC transformation can be induced by external stimuli such as light,⁴ heat,⁵ and guest molecules.⁶ During the SC-SC transformation, a significant rearrangement of molecular components in the crystals often takes place, resulting in changes of space group of single crystal and the coordination sphere of metal ions,⁷ thus the reservation of space group is not so common.⁸ Because the loss of single crystallinity occurs quite often after a drastic solid-state rearrangement of atoms, exploration of new MOFs that can endure the SC-SC transformations still remains a challenge. In porous 3D MOFs, water molecules are often used as terminal or bridging ligands.^{8b,9} By use of heat at a suitable temperature, loss of the terminal water ligands in 3D MOFs can occur in a SCSC transformation but removal of the bridging aqua ligands is more difficult.¹⁰ Until now, there has been only one report on SCSC transformation involving substitution of μ₂-bridging H₂O by an external solvent molecule through simultaneous bond breaking and

bond formation at RT in a 2D MOF.^{10c} In 3D MOFs, however, no example has been reported.

As a new generation of porous materials, MOFs possess high surface areas, large internal pore volumes and tunable pore sizes. However, many MOFs built from multicarboxylate-bridging ligands are prone to decomposition upon exposure to atmospheric water,^{11a} greatly limiting their industrial or commercial applications. Therefore, the design and exploitation of water stable MOFs are quite crucial for practical applications as functional materials.^{11b} To date, only few carboxylate-based porous MOFs materials have shown good stabilities toward water.¹² Moreover, the design and fabrication of porous MOFs materials that can selectively capture CO₂ is also of great interest due to the widespread public concern over global warming and climate change.^{12a} It has been found that some zeolitic imidazole frameworks (ZIFs) with polar -NO₂ group show high selectivity for capture of CO₂ and good stability toward water.^{11b} Our previous work revealed that 4,4'-biphenyldicarboxylic acid (H₂BPDC) with two methoxy groups, 2,2'(or 3,3')-dimethoxy-BPDC, can be used for construction of a series of MOFs with rich topology structures.¹³ Our current interest is to incorporate two -NO₂ groups into the BPDC backbone at the 2,2'-positions, and expect that the ligand, 2,2'-dinitro-BPDC (H₂L, Scheme 1a) can not only create robust MOFs with variable structures, but can also endow the MOFs with interesting properties. It is also noteworthy that only one example of 2D MOF based solely on H₂L ligand has recently been reported,¹⁴ albeit a few other MOFs based on the same ligand, but with the help of *N*-containing co-ligands, are known.¹⁵ On the basis of these considerations, we present herein the first 3D MOF [Cu₃L₂(μ₃-OH)₂(μ₂-H₂O)]·2DMA (**1**) based on H₂L ligand without any *N*-containing co-ligand. Remarkably, **1** can undergo irreversible solvent-induced SCSC transformations at RT when soaked in acetone, 2-propanol and 2-butanol, respectively, involving intramolecular substitution of μ₂-H₂O ligands and guest-exchanges by external solvent molecules. The SCSC transformations produce quantitatively three novel 3D MOFs: [Cu₃L₂(μ₃-OH)₂]·2S (**2A**, S = acetone; **2B**, S = 2-propanol; **2C**, S = 2-butanol) with their space groups being intact (Table S1, ESI†). Furthermore, reversible SCSC transformations by guest-exchanges among **2A**, **2B** and **2C** also take place at RT with their space groups all remaining unchanged (Scheme 1b). Such a solvent-induced substitution of μ₂-H₂O ligands in SCSC transformations at RT is unprecedented for the 3D

MOFs.^{6,10} In addition, **1** is a multifunctional microporous material due to its excellent separation selectivity of CO₂/N₂, good stability toward water and higher efficiency than the best-known ZIF-8 as a sorbent of μ -SPE.



Scheme 1 (a) Structure of ligand H₂L. (b) Irreversible SCSC transformations between **1** and **2(A, B, C)**, and reversible SCSC transformations among **2A, 2B** and **2C**.

Solvothermal reaction of Cu(NO₃)₂·3H₂O and H₂L with a metal-ligand ratio 3:2 in a binary solvent of DMA/H₂O led to the formation of **1** in 73.3% yield. Structural analysis reveals that **1** crystallizes in *P2₁/c* space group and the asymmetric unit (Fig. S1, ESI[†]) consists of three Cu²⁺ ions, two L²⁻ ligands, two μ_3 -OH⁻ ions, one μ_2 -H₂O and two DMA molecules. Both Cu1 and Cu2 are six-coordinated by a water molecule (O1W), two μ_3 -OH⁻ ions (O1ⁱ and O6) and three carboxyl oxygen atoms (O4ⁱⁱⁱ, O5ⁱⁱ, O18^{iv} for Cu1 and O3, O15, O16ⁱ for Cu2) with elongate octahedral geometries because the apical Cu-O bond lengths [2.449(5)-2.628(5) Å] are significantly longer than the basal ones [1.905(5)-1.994(4) Å] (Table S3, ESI[†]), while Cu3 is five-coordinated with a trigonal bipyramid geometry and its equatorial positions are defined by three carboxyl oxygen atoms (O2^v, O4ⁱⁱⁱ and O16) and the axial positions are occupied by two μ_3 -OH⁻ ions (O1 and O6). Notably, the equatorial Cu3-O distances [2.016(5)-2.215(4) Å] are slightly longer than the axial ones [1.908(4)-1.926(4) Å]. Three Cu²⁺ ions are linked together by μ_3 -OH⁻ ions and carboxyl groups to afford a novel trinuclear [Cu₃(μ_3 -OH)₂(-CO₂)₂]²⁺ motif (Fig. 1). The trinuclear Cu₃ motifs are interconnected by a μ_2 -H₂O and two $\mu_{1,1,3}$ -CO₂⁻ bridges to form an infinite 1D nanosized ribbon [Cu₃(μ_3 -OH)₂(μ_2 -H₂O)(-CO₂)₄]_n (8 Å) as rod-shaped SBU along the *c* axis (Fig. 2a). These 1D nanosized ribbons are further connected by the biphenyl groups of L²⁻ ligands forming a 3D framework (Fig. 2c). There are 1D rectangle channels of 10.864 × 10.484 Å² (excluding van der Waals radii) in **1** along the *c* axis (Fig. S2b, ESI[†]), which possess 40.2% solvent accessible voids occupied by DMA guest molecules (Fig. S2a, ESI[†]).

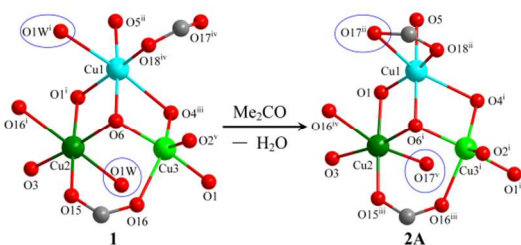


Fig. 1 The [Cu₃(μ_3 -OH)₂(-CO₂)₂]²⁺ motif in **1** and **2A**.

Single crystals of **1** (mother) exhibit a visible color change from light-blue to light-green (Fig. S3, ESI[†]) when immersed at RT in acetone, 2-propanol and 2-butanol, respectively, producing quantitatively three daughter single crystals, **2A-2C** with a general formula of [Cu₃L₂(μ_3 -OH)₂]-2S (**2: 2A**, S = acetone; **2B**, S = 2-propanol; **2C**, S = 2-butanol). All the three new crystals **2A-2C** adopt the same space group of **1** (Table S1, ESI[†]) and differ mainly

in guest molecules (Fig. S5, S6, ESI[†]). Because **2A-2C** have similar structural frameworks, herein, only the structure of **2A** is discussed in details. The asymmetric unit (Fig. S4, ESI[†]) of **2A** consists of three Cu²⁺ ions, two L²⁻ ligands, two μ_3 -OH⁻ ions and two acetone molecules. Both Cu1 and Cu2 adopt elongate octahedral geometries (Table S4, ESI[†]), while Cu3 is located at a trigonal bipyramid geometry. Two μ_3 -OH⁻ ions cap the triangular Cu₃ faces to form a trinuclear [Cu₃(μ_3 -OH)₂(-CO₂)₂]²⁺ core (Fig. 1) which are interconnected by the $\mu_{1,1,3}$ -CO₂⁻ bridges to form another infinite 1D nanosized ribbon [Cu₃(μ_3 -OH)₂(-CO₂)₄]_n (7 Å) along the *c* axis (Fig. 2b). The 1D nanosized ribbon is further linked through the biphenyl groups of L²⁻ ligands to generate a 3D network with 1D rectangle channels of 10.723 × 9.958 Å² (excluding van der Waals radii) along the *c* axis (Fig. 2c). These channels have 41% solvent accessible voids filled with acetone molecules (Fig. S5, ESI[†]). These features are very similar to those observed in **1**. However, two significant changes occurred during the SCSC transformation from **1** to **2A**: (1) all the μ_2 -H₂O molecules in **1** are completely removed in **2A**, (2) all the DMA in **1** have been totally replaced by acetone in **2A** as also confirmed by IR with the -C=O vibration of acetone appearing at 1737 cm⁻¹ (Fig. S9, ESI[†]). The changes directly result in a prominent decrease of the *b* axis in unit cell dimensions (34.135 Å in **1** vs. 32.500 Å in **2A**, Table S1, ESI[†]) and an indirect decrease of the 1D ribbon's width (8 Å in **1** vs. 7 Å in **2A**, Fig. 2a, 2b). Most importantly, an intrachain substituted reaction happens, resulting in a remarkable alteration of the local coordination environments of Cu1 and Cu2 in **2A**. The μ_2 -H₂O (O1W) molecules between Cu1 and Cu2 in **1** have been completely substituted by the adjacent uncoordinated carboxylate oxygen atoms (O17) via the formation of new coordinated bonds (Cu-O17 in **2A**) without change of the coordination numbers (Fig. 2b). Such a formation of new metal-carboxylate bonds during the SC-SC transformation without changing the space group and the coordination numbers of metal ions has not been observed for Cu(II)-MOFs^{3,10b,16} though some examples are known for the MOFs with Zn²⁺, Cd²⁺ and Ni²⁺ ions.^{7b,8a,17} Among the five reported SC-SC transformations involving release of μ_2 -H₂O molecules, four examples were triggered by heating^{10a-d} and the transformation at RT is very rare. In 2012, Sun *et al.* reported the example of SCSC transformations in a 2D MOF involving substitution of μ_2 -H₂O ligands by solvents at RT.^{10e} In that case, however, the SCSC transformation only involves replacements of the μ_2 -H₂O ligands by the external solvents (MeOH or DMSO) concomitant with change of space group, but no intramolecular substituted reaction occurs. To the best of our knowledge, the present SCSC transformation induced by the external solvents at RT involving loss of μ_2 -H₂O ligands and formation of new metal-carboxylate bonds without changing the space group is unprecedented. The unique structural transformation observed between **1** and **2** could be due to four reasons: (i) Cu(II) has variable coordination geometries and its Jahn-Teller's effect can facilitate the 1D nanosized ribbon distortion;^{10e} (ii) the H₂L ligands possess a flexible conformation (see change of the dihedral angles in Table S5, ESI[†]) and versatile coordination modes (Scheme S2, ESI[†]); (iii) the special topochemical geometry in **1**. The uncoordinated carboxylate oxygen atoms (O17) are close to the μ_2 -H₂O (O17...O1W = 4.794(3) Å)^{10b} and the axial Cu-O1W bonds are weak [Cu-O1W = 2.449(5), 2.628(5) Å]; (iv) hydrogen bond interactions between μ_2 -H₂O and DMA molecules may act as a 'double-edged sword'. On one hand, the intermolecular O1W-H1W...O hydrogen bond interactions in **1** (Fig. S7 and Table S6, ESI[†]) are helpful to the formation of the 1D nanosized ribbon and result in higher stability of the 3D framework before the SCSC transformation. On the other hand, the interactions

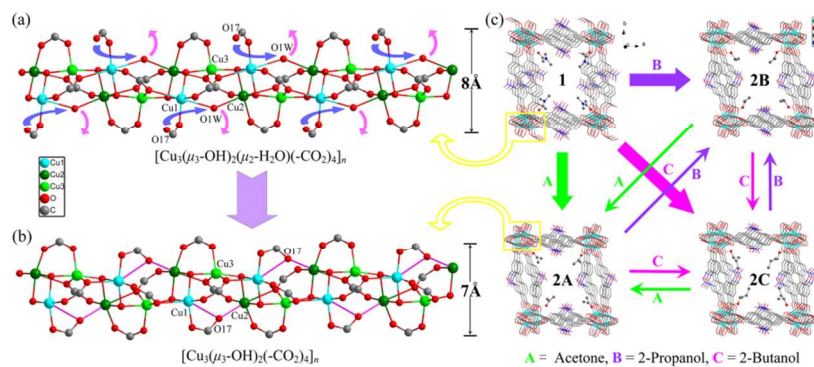


Fig. 2 The infinite 1D nanosized ribbon in **1** (a) and in **2A** (b). The significant changes from **1** to **2A** are highlighted. (c) The 3D frameworks of **1** and **2(A, B, C)** with 1D channels filled with solvent molecules shown in a ball-stick model along the *c* axis.

can also weaken the axial Cu-O1W bonds to some extent as soon as some polar solvents capable of forming hydrogen-bonding (acetone, 2-propanol and 2-butanol) approach. The weakness of the axial Cu-O1W bonds would be more beneficial to the removal of the μ_2 -H₂O and a shift of the adjacent uncoordinated carboxylate when the SCSC transformation can take place (a possible mechanism is proposed in ESI as a PPT file). Furthermore, the motif and polarity of the external guest molecules also play an important role because only the structural motif similar to 'Y'-type polar solvents such as acetone, 2-propanol and 2-butanol can induce the irreversible SCSC transformations of **1** to **2(A, B, C)**, while the other solvents like CH₂Cl₂, CHCl₃, CH₃CN, CH₃OH, C₂H₅OH, *n*-C₄H₉OH cannot initiate the transformations. Such a selective guest-responsive SCSC transformation may find potential applications in substrate-triggered sensor or shape-selective separation of positional isomers such as C₃ or C₄ alcohols.¹⁸ Further study on this field is currently in progress.

Notably, the daughter crystals **2A-2C** can be randomly interconverted (Fig. 2c) in SCSC fashion quantitatively by reversible guest-exchanges at RT without changes of space group and color (Table S2 and Fig. S3, ESI†). For example, dipping **2A** in 2-propanol for one day affords **2B** quantitatively, and when the crystal of **2B** is dipped in acetone for one day, **2A** is regenerated quantitatively. This type of reversible interconversion among **2A-2C** through guest-exchange SCSC transformations at RT is quite rare,^{8b,10e} and can be used to synthesize novel crystalline MOFs materials easily and quantitatively. Notably, none of the MOFs **2A-2C** could be obtained by direct solvothermal synthesis.

The experimental PXRD patterns of **1** and **2A** are basically identical to the respective simulated patterns, indicating the high phase purity of the bulk products of **1** and **2A** (Fig. S10, ESI†). When the crystals of **1** are immersed in water for one day, their peak positions are in good agreement with the simulated ones, revealing their good stability in water which is seldom observed in the carboxylate-based porous 3D MOFs materials.¹² The TGA curves (Fig. S11, ESI†) of **1** and **2A** show that the weight loss of 17.0% is observed from 38 to 253°C for **1** due to the loss of two DMA molecules and one coordinated μ_2 -H₂O (calculated 17.9%), and for **2A**, the weight loss of 10.6% occurs from 38 to 194°C due to the loss of two acetone molecules (calculated 11.6%).

To investigate the permanent porosity, **1** and **2A** were activated to obtain the fully evacuated framework. The N₂ adsorption isotherm of the guest-free samples at 77 K exhibited reversible type-I characteristics with a saturation uptake of 127 cm³/g for **1** and 190 cm³/g for **2A** (Fig. S12, ESI†). The estimated Brunauer-Emmett-Teller (BET) surface area was 395 m²/g for **1** and 596 m²/g for **2A** based on the N₂ sorption isotherm.

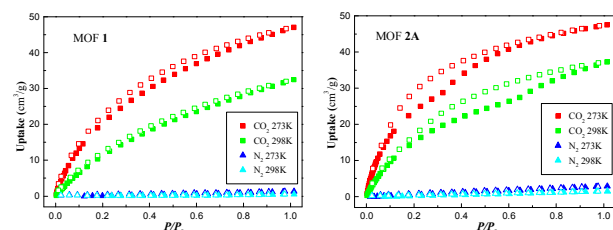


Fig. 3 Gas sorption isotherms for **1** and **2A** at 273 and 298 K. Solid symbols: adsorption; open symbols: desorption.

The pores of **1** and **2A** are densely functionalized with polar nitro groups directly exposed to channels (Fig. 2c). This unique feature prompted us to examine their CO₂ adsorption properties. The adsorption isotherms of CO₂ and N₂ for **1** and **2A** were measured up to 1 bar at 273 and 298 K, respectively. As shown in Fig. 3, the CO₂ and N₂ uptake values of **1** were 47.1 and 1.33 cm³/g at 273 K, and 32.5 and 0.52 cm³/g at 298 K, respectively, while the corresponding values of **2A** were 47.6 and 2.9 cm³/g at 273 K, and 37.2 and 1.5 cm³/g at 298 K, respectively. According to the conventional calculated method of initial slopes of adsorption isotherms,¹⁹ the selective separation ratio of CO₂/N₂ for **1** is 149 at 273 K and 128 at 298 K (Fig. S13, ESI†), while the corresponding value for **2A** is 116 at 273 K and 92 at 298 K (Fig. S14, ESI†). To our knowledge, the present separation selectivity of CO₂/N₂ for **1** is the highest value reported until now for MOFs materials at low pressures and under single-gas source conditions (Table S8, ESI†).^{12a,19} This apparent selectivity for CO₂ is presumably attributed to the interactions between CO₂ and the rich functional groups (-NO₂, μ_3 -OH⁻ and free -CO₂⁻) existed in **1**.^{11b,12a,15g} The high CO₂/N₂ separation selectivity and good water stability make **1** as a promising candidate for industrial post-combustion gas separation application.

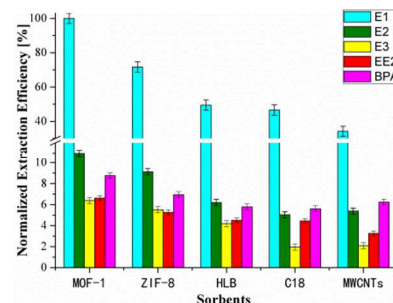


Fig. 4 Comparison of the normalized extraction efficiencies of **1**, ZIF-8 and commercial μ -SPE sorbents for five estrogens. The error bar shows standard deviation of the mean.

The good water stability and suitable pore size of **1** encouraged us to further study its possibility serving as a sorbent material for μ -SPE, a highly effective sample pretreatment and enrichment method for aqueous samples.²⁰ Our preliminary experimental results indicate that **1** shows higher extraction efficiency for five estrogens (Scheme S3, ESI†) than ZIF-8 (Fig. 4). Furthermore, no decrease of extraction performance was observed even after more than 10 replicated extractions (Table S9, ESI†). The PXRD peak positions of **1** after 10 extraction processes are in agreement with the as-synthesized ones (Fig. S10, ESI†), indicating an exceptional chemical stability of **1** in the μ -SPE experiments. Such excellent performance of **1** may result from its larger pore (12.7 Å) with bigger aperture (6.6 Å) than ZIF-8 (11.6 Å; 3.4 Å) and the possible hydrogen bonding interactions between the functional groups ($-\text{NO}_2$ and free $-\text{CO}_2^-$) in **1** and phenol group in the estrogens (Fig. S15, ESI†).²⁰

In summary, we have synthesized a smart single-crystal (**1**) by using a dinitro-substituted aromatic dicarboxylate ligand. **1** exhibits an unprecedented irreversible solvent-induced SC–SC transformation involving substitution of bridging water at RT through guest exchanges with acetone, 2-propanol, 2-butanol, producing quantitatively three daughter crystals (**2A–2C**). The **2A–2C** can also be quantitatively interconverted in SCSC fashion by reversible guest-exchange at RT. The good water and chemical stability, excellent separation selectivity of CO_2 over N_2 at RT, and higher extraction efficiency than ZIF-8 as a sorbent of μ -SPE make **1** as a potential multifunctional microporous MOF material.

This work was financially supported by the National Natural Science Foundation of China (Nos. 21171093, 21476115, 51109062).

Notes and references

^a State Key Laboratory of Materials-Oriented Chemical Engineering, College of Chemistry and Chemical Engineering, Nanjing Tech University, Nanjing, 210009, China

^b College of Environment, Hohai University, Nanjing, 210098, China

† Electronic Supplementary Information (ESI) available. CCDC 977429-977438. For ESI and crystallographic data in CIF or other electronic format see DOI: 10.1039/b000000x/

‡ These authors contributed equally to this work.

1 M. O’Keeffe and O. M. Yaghi, *Chem. Rev.*, 2012, **112**, 675.

2 Y. Cui, Y. Yue, G. Qian and B. Chen, *Chem. Rev.*, 2012, **112**, 1126.

3 J. J. Vittal, *Coord. Chem. Rev.*, 2007, **251**, 1781.

4 D. Liu, Z.-G. Ren, H.-X. Li, J.-P. Lang, N.-Y. Li and B. F. Abrahams, *Angew. Chem., Int. Ed.*, 2010, **49**, 4767.

5 T. Pretsche, K. W. Chapman, G. J. Halder and C. J. Kepert, *Chem. Commun.*, 2006, 1857.

6 (a) M. K. Sharma and P. K. Bharadwaj, *Inorg. Chem.*, 2011, **50**, 1889; (b) X.-P. Zhou, Z. Xu, M. Zeller, A. D. Hunter, S. S.-Y. Chui and C.-M. Che, *Inorg. Chem.*, 2011, **50**, 7142.

7 L. Wen, P. Cheng and W. Lin, *Chem. Commun.*, 2012, **48**, 2846.

8 (a) J. D. Ranford, J. J. Vittal and D. Wu, *Angew. Chem., Int. Ed.*, 1998, **37**, 1114; (b) M. C. Das and P. K. Bharadwaj, *J. Am. Chem. Soc.*, 2009, **131**, 10942.

9 X.-Y. Dong, B. Li, B.-B. Ma, S.-J. Li, M.-M. Dong, Y.-Y. Zhu, S.-Q. Zang, Y. Song, H.-W. Hou and T. C. W. Mak, *J. Am. Chem. Soc.*, 2013, **135**, 10214.

10 (a) D.-X. Xue, W.-X. Zhang, X.-M. Chen and H.-Z. Wang, *Chem. Commun.*, 2008, 1551; (b) S. K. Ghosh, W. Kaneko, D. Kiriya, M.

Ohba and S. Kitagawa, *Angew. Chem., Int. Ed.*, 2008, **47**, 8843; (c) Y. Fu, J. Su, S. Yang, Z. Zou, G. Li, F. Liao, M. Xiong and J. Lin, *Cryst. Growth Des.*, 2011, **11**, 2243; (d) D. L. Reger, A. Leitner, M. D. Smith, T. T. Tran and P. S. Halasyamani, *Inorg. Chem.*, 2013, **52**, 10041; (e) G.-C. Lv, P. Wang, Q. Liu, J. Fan, K. Chen and W.-Y. Sun, *Chem. Commun.*, 2012, **48**, 10249.

11 (a) P. Kùsgens, M. Rose, I. Senkovska, H. Fròde, A. Henschel, S. Siegle and S. Kaskel, *Microporous Mesoporous Mater.*, 2009, **120**, 325; (b) R. Banerjee, H. Furukawa, D. Britt, C. Knobler, M. O’Keeffe and O. M. Yaghi, *J. Am. Chem. Soc.*, 2009, **131**, 3875.

12 (a) Q. Yang, S. Vaesen, F. Ragon, A. D. Wiersum, D. Wu, A. Lago, T. Devic, C. Martineau, F. Taulelle, P. L. Llewellyn, H. Jobic, C. Zhong, C. Serre, G. D. Weireld and G. Maurin, *Angew. Chem., Int. Ed.*, 2013, **52**, 10316; (b) Q. Chen, Z. Chang, W.-C. Song, H. Song, H.-B. Song, T.-L. Hu and X.-H. Bu, *Angew. Chem., Int. Ed.*, 2013, **52**, 11550.

13 (a) X.-Z. Wang, D.-R. Zhu, Y. Xu, J. Yang, X. Shen, J. Zhou, N. Fei, X.-K. Ke and L.-M. Peng, *Cryst. Growth Des.*, 2010, **10**, 887; (b) H.-J. Zhang, X.-Z. Wang, D.-R. Zhu, Y. Song, Y. Xu, H. Xu, X. Shen, T. Gao and M.-X. Huang, *CrystEngComm*, 2011, **13**, 2586; (c) H. Xu, W. Bao, Y. Xu, X. Liu, X. Shen and D. Zhu, *CrystEngComm*, 2012, **14**, 5720; (d) R. Luo, H. Xu, H.-X. Gu, X. Wang, Y. Xu, X. Shen, W. Bao and D.-R. Zhu, *CrystEngComm*, 2014, **16**, 784.

14 J.-Y. Zhang, X.-B. Li, K. Wang, Y. Ma, A.-L. Cheng and E.-Q. Gao, *Dalton Trans.*, 2012, **41**, 12192.

15 (a) J.-Y. Zhang, X.-H. Jing, Y. Ma, A.-L. Cheng and E.-Q. Gao, *Cryst. Growth Des.*, 2011, **11**, 3681; (b) B. Li, G. Li, D. Liu, Y. Peng, X. Zhou, J. Hua, Z. Shi and S. Feng, *CrystEngComm*, 2011, **13**, 1291; (c) B. Li, Y. Zhang, G. Li, D. Liu, Y. Chen, W. Hu, Z. Shi and S. Feng, *CrystEngComm*, 2011, **13**, 2457; (d) B. Li, X. Zhou, Q. Zhou, G. Li, J. Hua, Y. Bi, Y. Li, Z. Shi and S. Feng, *CrystEngComm*, 2011, **13**, 4592; (e) J.-Y. Zhang, Y. Ma, A.-L. Cheng, Q. Yue, Y. Q. Sun and E.-Q. Gao, *Dalton Trans.*, 2011, **40**, 7219; (f) B. Li, F. Yang, Y. Zhang, G. Li, Q. Zhou, J. Hua, Z. Shi and S. Feng, *Dalton Trans.*, 2012, **41**, 2677; (g) P. V. Dau and S. M. Cohen, *CrystEngComm*, 2013, **15**, 9304.

16 N. Masciocchi, S. Galli, G. Tagliabue, A. Sironi, O. Castillo, A. Luque, G. Beobide, W. Wang, M. A. Romero, E. Barea and J. A. R. Navarro, *Inorg. Chem.*, 2009, **48**, 3087.

17 (a) M. Nagarathinam and J. J. Vittal, *Chem. Commun.*, 2008, 438; (b) A. Calderón-Casado, G. Barika, B. Bazán, M.-K. Urriaga, O. Vallcorba, J. Rius, C. Miravittles and M.-I. Arriortua, *CrystEngComm*, 2011, **13**, 6831.

18 (a) T. Mitra, K. E. Jelfs, M. Schmidtman, A. Ahmed, S. Y. Chong, D. J. Adams and A. I. Cooper, *Nature Chem.*, 2012, **5**, 276; (b) T. Jacobs, G. O. Lloyd, J. A. Gertenbach, K. K. Mueller-Nederbock, C. Esterhuysen and L. J. Barbour, *Angew. Chem., Int. Ed.*, 2012, **51**, 4913; (c) Y. Takashima, V. M. Martínez, S. Furukawa, M. Kondo, S. Shimomura, H. Uehara, M. Nakahama, K. Sugimoto and S. Kitagawa, *Nature Commun.*, 2011, **2**, 168.

19 J. An, S. J. Geib and N. L. Rosi, *J. Am. Chem. Soc.*, 2010, **132**, 38.

20 Y. Wang, S. Jin, Q. Wang, G. Lu, J. Jiang and D. Zhu, *J. Chromatogr. A*, 2013, **1291**, 27.